Asian Journal of Chemistry; Vol. 35, No. 12 (2023), 3013-3021

ASIAN JOURNAL OF CHEMISTRY

https://doi.org/10.14233/ajchem.2023.30578

Synthesis and Characterization of Peppermint Oil Loaded Complex Coacervates of Chitosan Phosphate/κ-Carrageenan and Evaluation of their Antibacterial Activity

A. SARMA[1], J. RABHA[2], M. UPADHYAYA[3] and D.K. KAKATI[1,*]

[1]Department of Chemistry, Gauhati University, Guwahati-781014, India
[2]Department of Botany, Gauhati University, Guwahati-781014, India
[3]Department of Chemistry, Chayduar College, Gohpur-784168, India

*Corresponding author: E-mail: dkk.chem@gauhati.ac.in

Received: 27 September 2023; *Accepted*: 28 October 2023; *Published online*: 2 December 2023; AJC-21463

Peppermint oil has been in use as traditional medicine for several common ailments besides being used as flavourings in foods and beverages. Like other essential oils it is also susceptible to oxidative degradation on exposure to oxygen, light and heat, which results in its decreased shelf life. Complex coacervation is a commonly used technique to encapsulate essential oils to give protection against degradation as well as providing a carrier vehicle for sustained release. In present work, the peppermint oil was encapsulated in a complex coacervate from a chitosan derivative, chitosan phosphate and κ-carrageenan in the presence of glutaraldehyde as crosslinking agent. The reaction conditions were optimized .The highest yield of the coacervate was recorded at pH 4.6 of the reaction medium and at a ratio of 2:4 by volume of 0.3% (w/v) solution of chitosan phospahate and κ-carrageenan. The effect of the variation of amount of crosslinker on the morphology and swelling property of the coacervate was also investigated and both the properties were found to be affected. A maximum loading efficiency of 84.19% was observed. The swelling and release studies revealed that both were pH dependent and release of peppermint oil from the coacervate showed a sustained release profile over a period of 72 h. The peppermint oil loaded coacervates were investigated for their antibacterial activities against *Micrococcus luteus*, *Staphylococcus epidermidis*, *Escherichia coli*, *Klebsiella pneumonia* and *Proteus vulgarus* and found to be mildly effective against all of them.

Keywords: Peppermint oil, Chitosan phosphate, κ-Carrageenan, Antibacterial activity.

INTRODUCTION

Essential oils are naturally available plant based oils, characterized by their distinct aromas. A few common essential oils are peppermint, lavender, patchouli, tea-tree, eucalyptus, lemon, lemon grass, citronella, *etc*. The essential oils mainly contain terpenoid hydrocarbons and their derivatives, and many flavonoids and phenolic compounds. Peppermint (*Mentha piperita*) is a well-known member of *Lamiaceae* family and the oil is extracted from the leaves [1]. The main active components of the oil accountable for its aroma, flavour and cool feeling on contact are menthol, menthone and menthyl acetate [2]. Peppermint oil has therapeutic value in the treatment of several common ailments. It is useful in the treatment of various digestive ailments such as Crohn's disease, irritable bowel syndrome [3], liver and gall bladder complaints, diverticulitis, loss of appetite, gas, bloating, diarrhea, *etc*. [4]. It is reported to help relieve spastic colon, diarrhea and eases nausea and vomiting [5]. Stress, insomnia, restlessness and anxiety are also treated with peppermint oil. But peppermint oil like many other essential oils is volatile in nature and is prone to oxidative degradation under environmental conditions.

Complex coacervate based microencapsulation can protect it against environmental degradation as well as facilitate its targeted delivery for therapeutic action [6]. Literature has several reports on the encapsulation of peppermint oil in protective ensembles. For example, Dong *et al*. [7] encapsulated peppermint oil in a complex coacervate microcapsules prepared from gelatin and gum Arabic hardened with *trans*-glutaminase. The capability of lipid based micro and nano particles to load and release of loaded peppermint oil in a slow manner was investigated by Yang & Ciftci [8]. Peppermint oil loaded gelatin/gum Arabic microcapsules prepared by Dong *et al*. [9] were investigated for the release of the encapsulated oil in different

dispersing mediums and found the release to be very slow in cold water. Cellulose nanocrystals based carrier for peppermint oil was investigated by Kasiri & Fathi [10] for applications in pharmaceuticals and food. Peppermint oil was also encapsulated in chitosan/alginate polyelectrolyte complex in the presence of glutaraldehyde as crosslinker as reported by Deka *et al*. [11]. They optimized the reaction conditions of coacervate formation and the loading of oil. The peppermint oil loaded polyelectrolyte complexes exhibited the excellent antibacterial activities against *Staphylococcusaureus*, *Enterobacter aerogenes*, *Proteus mirabilis* and *Bacillus subtilis*. Ghayempour & Montazer [12] synthesized peppermint oil loaded *Tragacanth* nanofibres by microemulsion method. The prepared nanofibres were smooth with thickness of 58 nm. A controlled release pattern was observed and after 18 h, the release of the peppermint oil from the *Tragacanth*nano fibres was 92.38 %. High antibacterial activity was shown against *E. coli* and *S. aureus*. Liu *et al*. [13] prepared peppermint oil loaded starch nanoparticles through ultrasonic bottom-up technique. The encapsulation efficiency and loading capacity were reported as 87.7% and 25.5%, respectively. Shetta *et al*. [14] prepared the chitosan nanoparticles and encapsulated peppermint oil and green tea oil using ionic gelation method. The encapsulation efficiency of 78-82% for peppermint oil and 22-81 % for green tea oil was reported. The loaded nanoparticles also showed effective antibacterial activity against *E. coli* and *S. aureus*. Parkzad *et al*. [15] used tannic acid as crosslinker in the preparation of gelatin and gum Arabic based complex coacervate for encapsulation and release studies of peppermint oil.

Chitosan is a material of choice for synthesis of complex coacervates with several anionic macroions. However, chitosan derivatives are found to have better aqueous solubility profile than chitosan. Therefore, the use of chitosan derivatives in place of chitosan is gradually attracting the interest in the development encapsulating systems [16]. The present work reports the use of a chitosan derivative chitosan phosphate in the preparation of a complex coacervate with κ-carragennan and its subsequent use in the encapsulation of peppermint oil. The pH dependency of release of peppermint oil was investigated and the effectiveness of peppermint oil loaded coacervate was investigated against a few Gram-positive and Gram-negative bacterial strains.

EXPERIMENTAL

Low molecular weight chitosan (75-85% deacetylated, Sigma-Aldrich, USA), κ-carrageenan (Sigma-Aldrich, USA), peppermint oil (Sigma-Aldrich, USA), glutaraldehyde (E. Merck, India) were purchased and used as received. Ethanol was procured from Merck (India). Inhibition zone scale (Himedia, India), nutrient broth (Himedia, India) and DMSO (Merck, India) were also used. The bacterial strains, *Micrococcus luteus* (ATCC 4638), *Staphylococcus epidermidis* (ATCC 12228), *Escherichia coli* (ATCC 1705), *Klebsiella pneumonia* (ATCC 1705), *Proteus vulgarus* (MTCC 743) were procured from the Institute of Microbial Technology, Chandigarh, India. All other reagents were of analytical grade and used without further purification. Deionized water was used in all the experiments.

Preparation of chitosan phosphate: Chitosan phosphate was prepared by a reported method as described [17]. Briefly, 2 g chitosan was dissolved in 100 mL 2% acetic acid solution and after addition of 6 g orthophosphoric acid, the reaction mixture was refluxed for 2 h. It was then cooled and poured into excess methanol. The white product formed was dissolved in minimum volume of water and reprecipitated in excess methanol. The product chitosan phosphate was then dried in a vacuum oven at 80 ºC and stored.

Formation of complex coacervate: The electrostatic interaction between the cationic chitosan phosphate and anionic κ-carrageenan resulted in the formation of a complex coacervate which then separated from the aqueous solution. The degree of ionization of the two constituents depends on the pH of the reaction medium and hence pH is a determining factor in the complex formation process. Secondly, the complex formation also depends on the ratio of concentration of two constituents. Hence, the pH of medium and ratio of the concentration of two components are required to be optimized to get the maximum yield of the coacervate.

Determination of optimum pH of reaction media: Buffer solutions of nine different pHs (3.6, 3.8, 4.0, 4.2, 4.4, 4.6, 4.8, 5.0, 5.2) were prepared by using 0.1N acetic acid and 0.1N sodium acetate solutions. 0.75 g of κ-carrageenan was dissolved in 250 mL buffer of specific pH to prepare a solution of concentration 0.3% by (w/v). Similalrly, 0.75 g chitosan phosphate was dissolved in 250 mL buffer of the same pH by stirring at 30 ºC to prepare a solution of concentration 0.3% w/v. Carrageenan solution was added dropwise to chitosan phosphate solution under stirring at room temperature. This procedure was followed in buffer solutions of nine different pH. The coacervates formed were dried in vacuum oven at 40 ºC till constant weights were obtained.

Determination of optimum ratio of chitosan phosphate to κ-carrageenan: To determine the optimum ratio of two constituents, the coacervation reactions were done with varying ratio of them in buffer of pH 4.6 as it was found to be the optimum pH giving the maximum yield. The 0.3%(w/v) solutions of chitosan phosphate and κ-carrageenan were used for the purpose. Maintaining a total volume of 30mL, carrageenan and chitosan phosphate solutions were mixed at five different volume ratios at room temperature. The ratios were 25:5, 20:10, 15:15, 10:20, 5:25, respectively. The optimum ratio resulting in the maximum yield of coacervate was determined by measuring the weights of the coacervates formed and by measuring the viscosity and conductivity of the supernatant liquid.

Swelling studies: Swelling of the coacervates was investigated in mediums of pH 4, 7, 7.4 and 9. Known weights of the coacervates were immersed in solutions of four different pH. After definite time intervals, the weights of swollen coacervates were measured and this process was continued for 72 h. The equilibrium swelling index was then calculated from eqn. 1 [18]:

$$\text{Swelling index } (\%) = \frac{W_g - W_o}{W_o} \times 100 \qquad (1)$$

where W_g = weight of coacervate after swelling, W_o = weight of coacervate before swelling.

Preparation of peppermint oil loaded chitosan phosphate/carrageenan coacervate: Peppermint oil was loaded into chitosan phosphate/carrageenan coacervate by carrying out the coacervation reaction in presence of peppermint oil, at pH 4.6 and maintaining the ratio of 0.3% (w/v) solutions of chitosan phosphate and κ-carrageenan at 2:4. The required amount of peppermint oil was added drop wise to the carrageenan solution under stirring. This is followed by the dropwise addition of mixture of carageenan and peppermint oil to the chitosan phosphate solution. After complete addition, it was stirred for about 1.5 h by maintaining the temperature at around 45 ºC. The reaction mixture was then cooled to around 15 ºC and the crosslinker glutaraldehyde was added followed by stirring of the reaction mixture for another 1.5 h at 45 ºC. The resultant product was filtered, washed with copious amount of ethanol and freeze dried.

Preparation of calibration curve for peppermint oil: To determine the amount of peppermint oil encapsulated in the coacervate and released from it, a calibration curve was plotted for peppermint oil. A series of dilute solutions were prepared by dissolving known amount of peppermint oil in ethanol. The solutions were scanned in the range of 200-450 nm in a UV-visible spectrophotometer (UV-1800, Shimadzu). Absorptions at wavelength 227 nm were plotted against the concentration of the peppermint solution. A straight line was obtained with y=17.437*x* + 0.0082 and R^2 = 0.9987 as shown in Fig. 1.

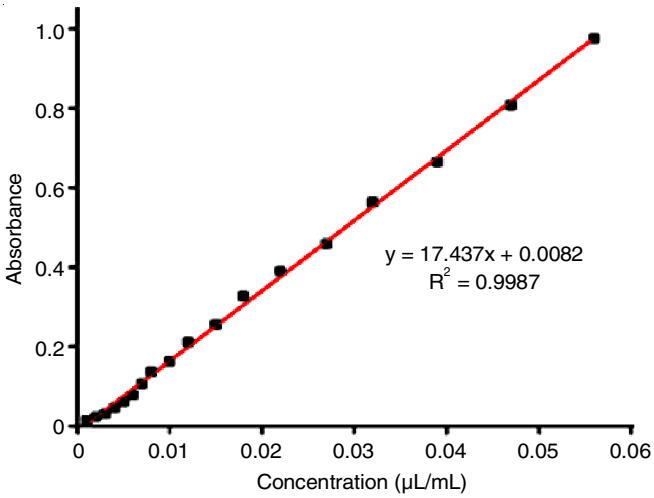

Fig. 1. Calibration curve of peppermint oil

Loading efficiency: The peppermint oil loaded coacervates were agitated in ethanol to extract the oil in ethanol. The oil was quantified spectrophotometrically in a UV-Vis spectrophotometer (Shimadzu, Japan) at 227 nm. Loading efficiency (LE) was calculated by using eqn. 2 [11] with different amount of peppermint oil during synthesis as shown in Table-1.

$$\text{LE (\%)} = \frac{\text{Total amount of peppermint oil loaded in the coacervate}}{\text{Total amount of peppermint oil taken}} \times 100 \quad (2)$$

TABLE-1
LOADING EFFICIENCY OF THE COACERVATE

Peppermint oil (mL)	Glutaraldehyde (mL)	Loading efficiency (%)
0.5	1.0	45.69
0.8	1.0	84.19
1.0	1.0	62.59
1.5	1.0	53.42
0.8	0.5	50.29
0.8	1.5	48.36
0.8	2.0	42.34
0.8	2.5	38.18

Release studies: Release of peppermint oil from the coacervate was investigated at pH 4, 7 and 9 and 7.4 for a period of 72 h. The percentage of peppermint oil released from the coacervates was then determined by using eqn. 3 [19]:

$$\text{Release (\%)} = \frac{\text{Released peppermint oil from coacervate}}{\text{Total amount of peppermint oil in the coacervate}} \times 100 \quad (3)$$

Antibacterial activity assay: The antibacterial activity of peppermint oil loaded coacervate was evaluated against five different bacterial strains *viz*. *Micrococcus luteus*, *Escherichia coli*, *Staphylococcus epidermidis*, *Klebsiella pneumonia* and *Proteus vulgarus* by Agar well-diffusion method (Kirby-Bauer diffusion method) [20]. The microorganisms were cultured for 24-48 h in nutrient broth at 28 ± 1 ºC. In the agar well, the samples, tetracycline as positive control and DMSO as negative control were incubated at 28 ± 1 ºC and for 4 to 7 days. At the end of the incubation period zones of inhibition were measured.

RESULTS AND DISCUSSION

Optimization of reaction parameters for preparing coacervate: Weights of the coacervates formed at different pH were measured and it was found that the maximum yield of coacervate was recorded at pH 4.6 (Fig. 2a). At pH 4.6, the optimum ratio of κ-carrageenan and chitosan phosphate at the concentration 0.3% (w/v) was 20:10 or 1:2. Fig. 2b-d show the plot of variation of the weights of coacervate and the time of flow (viscosity) and conductivity of the supernatant liquid against the ratio by volume of 0.3% (w/v) solution of κ-carrageennan and chitosan phosphate.

FTIR studies: The FTIR spectra (Shimadzu IR Affinity-1 spectrophotometer) were recorded within the scanning range of 4000-400 cm^{-1} using KBr pellets. Chitosan (Fig. 3a) showed peaks at 3462 cm^{-1} (-OH and N-H *str.*), 1643 cm^{-1} (C=O *str*. of amide I), 1554 cm^{-1} (N-H *bend*. of amide II), 1415 cm^{-1} (C-N *str*. amide III) and 1078 cm^{-1} (C-O-C *str.*) [21,22]. Carrageenan showed peaks at 3419 cm^{-1} (O-H *str.*), 2919 cm^{-1} (CH_3 sym., CH_2 asym.), 1421 cm^{-1} (CH_3, CH_2 bend.), 1373 cm-1 (sulfonic acid groups), 1261 cm^{-1} (C-O *str.*), 1072 cm^{-1} (C-O (-C-OH-) vibration) and 848 cm^{-1} (sulfation of C4 of β-1,3-linked residue) [23]. Chitosan phosphate (Fig. 3b) showed peaks at 3473 cm^{-1} (-OH group), 1645 cm^{-1} (asym. N-H *bend*. of amide I), 1550 cm^{-1} (sym. N-H *bend*. of amide II), 1309 cm^{-1} (P=O *str.*), 1078 cm^{-1} (phosphorylated hydroxyl groups) and 520 cm^{-1} (P-OH group) [24]. The unloaded coacervate showed peaks at 3466, 1652, 1560, 1419 and 1076 cm^{-1}. Most of the peaks due to chitosan phosphate and carrageenan are present in the coac-

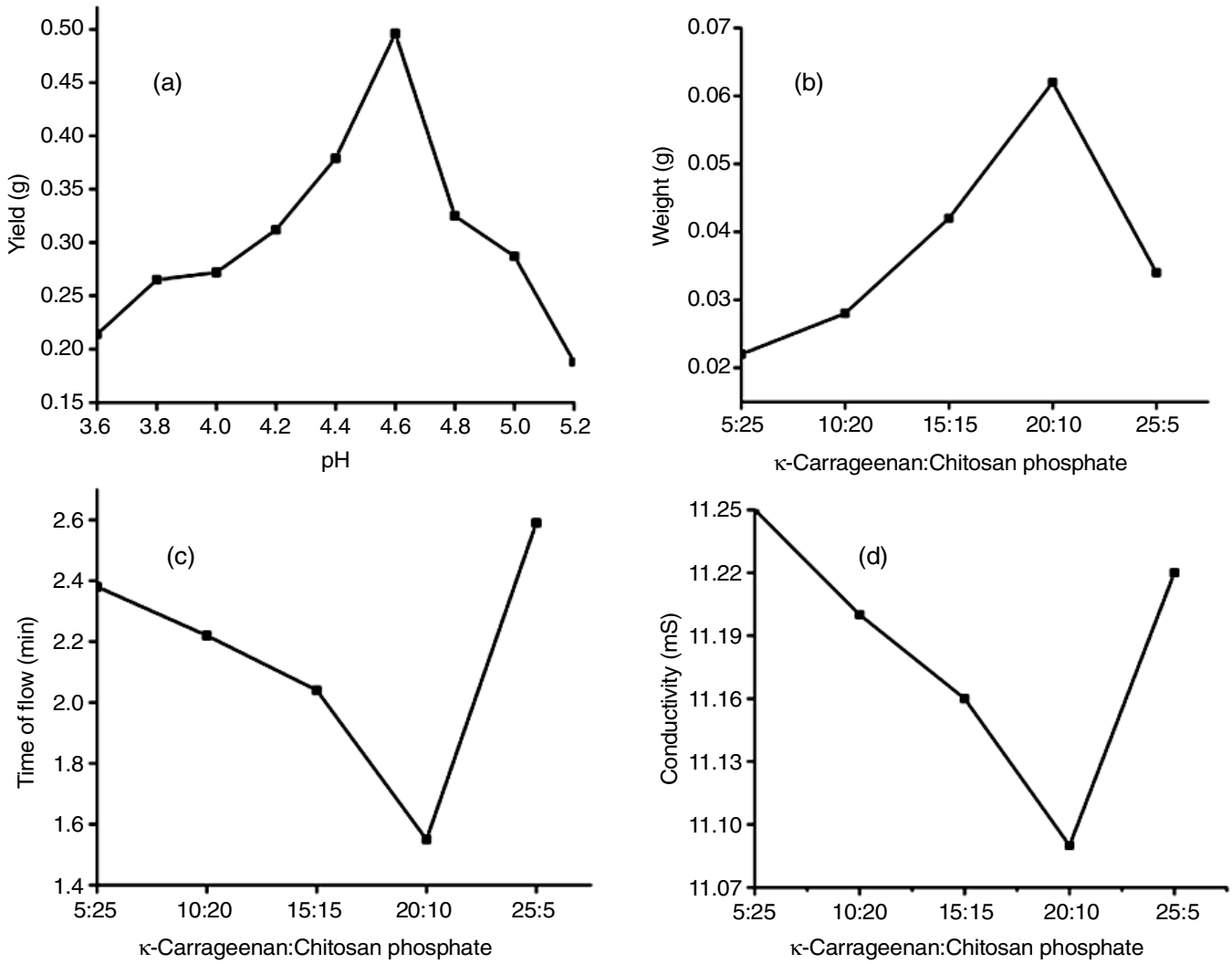

Fig. 2. (a) Variation of yield of the coacervate with pH, variation of (b) yield of the coacervate and (c) viscosity (d) conductivity of the supernatant liquid against the ratio by volume of 0.3% (w/v) solution of carragennan and chitosan phosphate

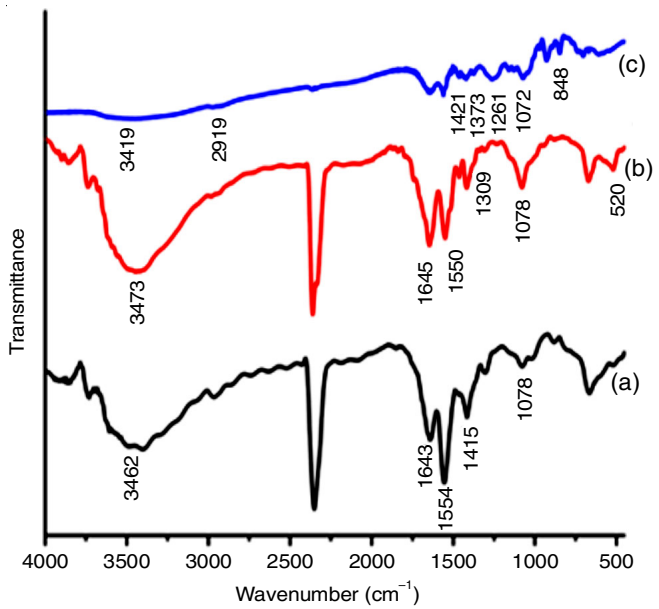

Fig. 3. FTIR spectra of (a) chitosan (b) chitosan phosphate and (c) κ-carrageenan

ervate with minor change in the shape and shift of absorption values (Fig. 4a). This is due to protonation of the NH_2 group in chitosan phosphate and electrostatic interaction between chitosan phosphate and carrageenan. Peppermint oil (Fig. 4b) showed peak at 3452 cm^{-1} (-OH), 2924 cm^{-1} (-CH_3), 2868 cm^{-1} (-CH_2), 1707 cm^{-1} (C=O). The peaks at 1456 and 1381 cm^{-1} were due to the C-H bending, while the peaks at 1043 and 1028 cm^{-1} were due to the C-O vibration [25]. Further, the loaded coacervate showed peaks at 3452, 2935, 2866, 1716, 1633, 1384 and 1066 cm^{-1} (Fig. 4c). The major peaks due to chitosan phosphate/carrageenan coacervate are present, however with slight shift in their absorption frequencies, which may be due to interaction with peppermint oil.

Variation in the concentration of crosslinker glutaraldehyde affects the microstructure of coacervate as revealed by in Fig. 5. The FTIR spectra recorded for the coacervate with 2.5 mL glutaradehyde showed a strong and broad peak centered at 1587 cm^{-1} [26] (Fig. 5a). This is either weak or merged with other peaks in the sample with 0.5 mL of glutaraldehyde in the reaction (Fig. 5b). The other possibility

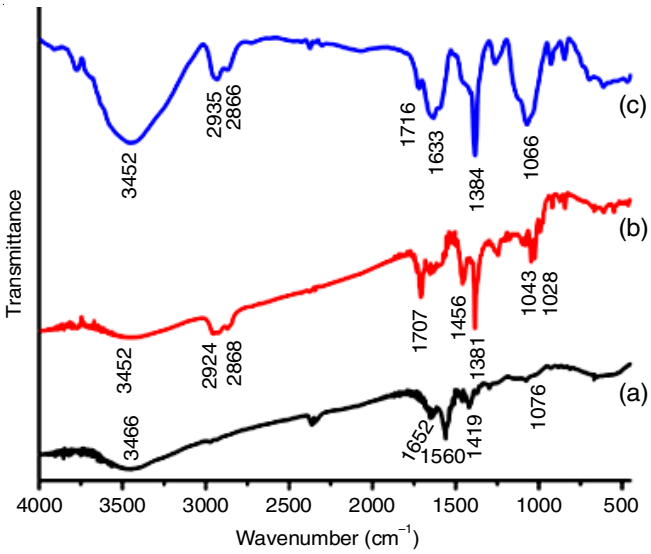

Fig. 4. FTIR spectra of (a) coacervate, (b) peppermint oil and (c) peppermint oil loaded coacervate

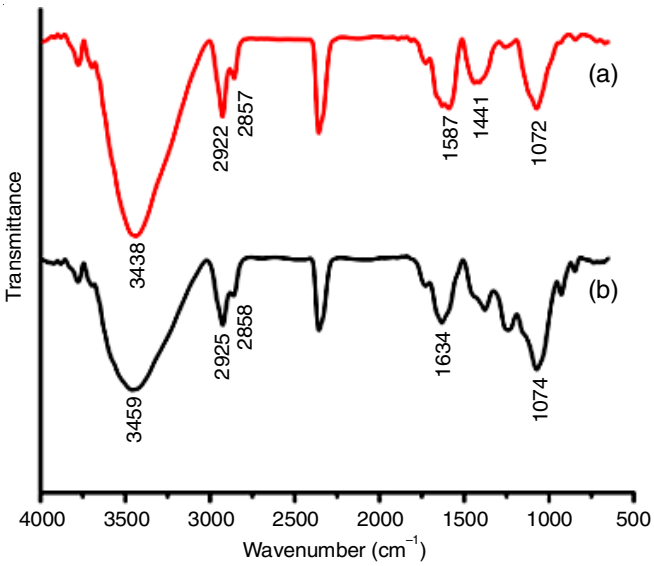

Fig. 5. FTIR spectra of peppermint oil loaded CP/carrageenan coacervate with two different amounts of glutaraldehyde [0.5 mL (b) and 2.5 mL (a)]

is the formation of an amide bond with acidic functionality of κ-carragennan with peaks in the range of 1640-1550 cm^{-1} [27].

TGA studies: Thermogravimetric analysis was done in a Perkin-Elmer TGA 4000 in the temperature range of 30-700 ºC at a heating rate of 10 ºC/min under nitrogen flow of 20 mL/min. Chitosan showed a two steps thermal degradation, where the first weight loss in chitosan took place at around 45-100 ºC due to loss of absorbed water molecules (Fig. 6). The major weight loss in chitosan took place at around ~300 ºC [28] due to breakdown of polymer backbone. On the other hand, the main weight loss for chitosan phosphate was observed at around ~200 ºC (Fig. 6b), indicating a decrease in thermal stability of chitosan phosphate with respect to chitosan, resulting from the phosphorylation of the primary alcoholic groups of chitosan [17]. Introduction of bulky phosphate group is probably affecting the close packing of the individual polysaccharide chains. For κ-carrageenan (Fig. 6c), the two weight loss phenomena were observed at ~210 and 240 ºC, respectively. The first weight loss may be due to the removal of acid functionalities while second one started at 240 ºC indicated the gradual degradation of the backbone structure [23]. The complex coacervate exhibited a different degradation pattern than the constituting components indicating the formation of a new material (Fig. 6d). Besides the weight loss due to loss of moisture, it exhibited two other weight losses at ~300 and ~500 ºC, respectively .The loading of peppermint oil resulted in a change in the weight loss pattern of the coacervate, indicating the influence exerted by oil in the thermal behaviour of the coacervate, with the major weight loss taking place at around 250 ºC (Fig. 6e).

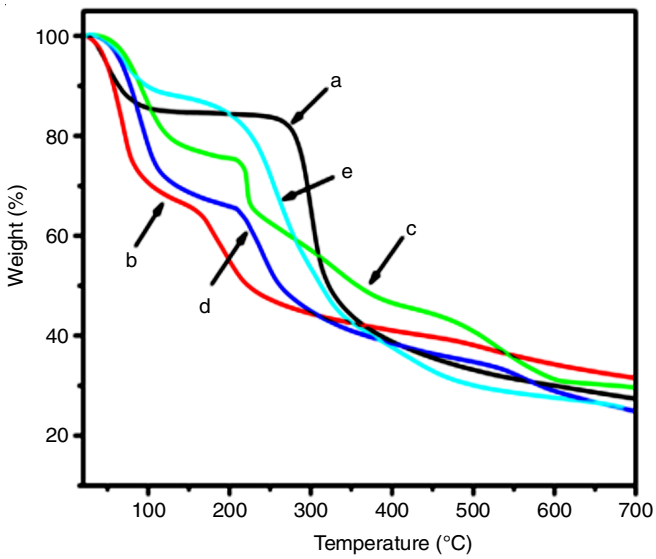

Fig. 6. Thermogravimetric curves of (a) chitosan, (b) chitosan phosphate, (c) carrageenan, (d) coacervate and (e) peppermint oil loaded coacervate

Swelling study: The swelling index (%) of the coacervates against time is presented in Fig. 7. The coacervates were found to swell quickly in the first 6 h of soaking. After that swelling decreases and attained an equilibrium swelling value after 24 h. Swelling was pH dependent in nature and attained maximum and minimum at pH 9 and 4, respectively. The protonation of the amino groups of chitosan phosphate is pH dependent and increases with reduction in the pH of medium. With increase in the degree of protonation electrostatic interaction with the κ-carrageenan increases. These interactions bound the polymers together resulting in tight network and so swelling showed a downward trend with the lowering pH. But in alkaline medium deprotonation of chitosan phosphate increases resulting in the weakening of the electrostatic interactions between κ-carrageenan and chitosan phosphate. Moreover, there will be repulsion between the sulphate groups of κ-carrageenan. All these result in loosening of the network structure leading to increase in swelling [29,30].

Effect of amount of crosslinker on swelling: Crosslinker has a pronounced effect on swelling. Coacervates were prepared with varying amounts of crosslinker, glutaraldehyde (0.5, 1, 1.5,2 and 2.5 mL) and swelling was observed for a period of 72 h in medium of pH, 4, 7, 7.4 and 9. With rise in the amount

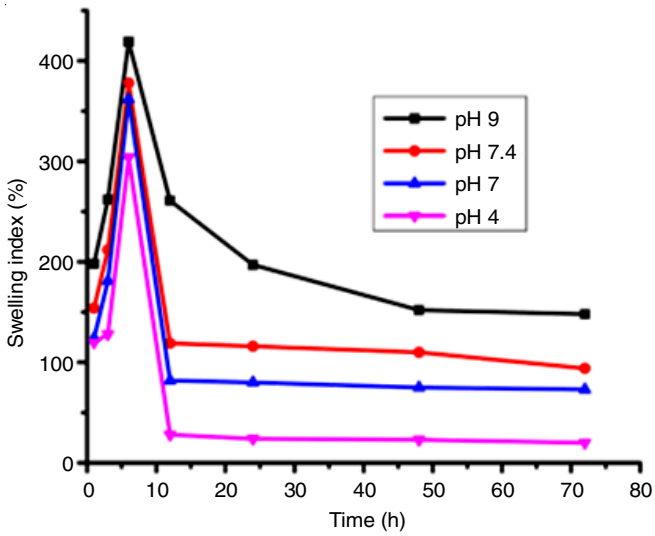

Fig. 7. Swelling index (%) coacervate at pH 4, 7, 7.4 and 9

of glutaraldehyde, swelling decreases, which is attributed due to more compact structure of the coacervate resulting with the increase in amount of glutaraldehyde (Fig. 8). Similar observation was reported by Distantina *et al.* [31] while preparing glutaraldehyde crosslinked κ-carrageenan hydrogels.

Morphology studies: The effect on the morphology of the coacervate with the increase in the amount of crosslinker was also investigated by scanning electron microscopy. The micrographs (Fig. 9), clearly demonstrated that as the amount of cross-linker increased, the morphology of the material exhibited a more particulate nature, accompanied by an increase in particle sizes.

Loading efficiency: Loading efficiencies (LE) for different amounts of peppermint oil in the loading solution were calculated and the values are shown in Table-1. With increase in the amount of peppermint oil, loading efficiency increased and after attaining a maximum value (84.19%), it started decreasing. This is because the coacervate has a limit to its ability to load. If the amount of peppermint oil in the loading solution is further increased then loading efficiency decreased as expected from the expression for calculating the LE (%). In this case, the maximum loading efficiency observed was 84.19% with 0.8 mL peppermint oil in the loading solution with 1.0 mL cross-linker. The effect of the amount of cross-linker glutaraldehyde in the preparation of coacervate also influences the loading

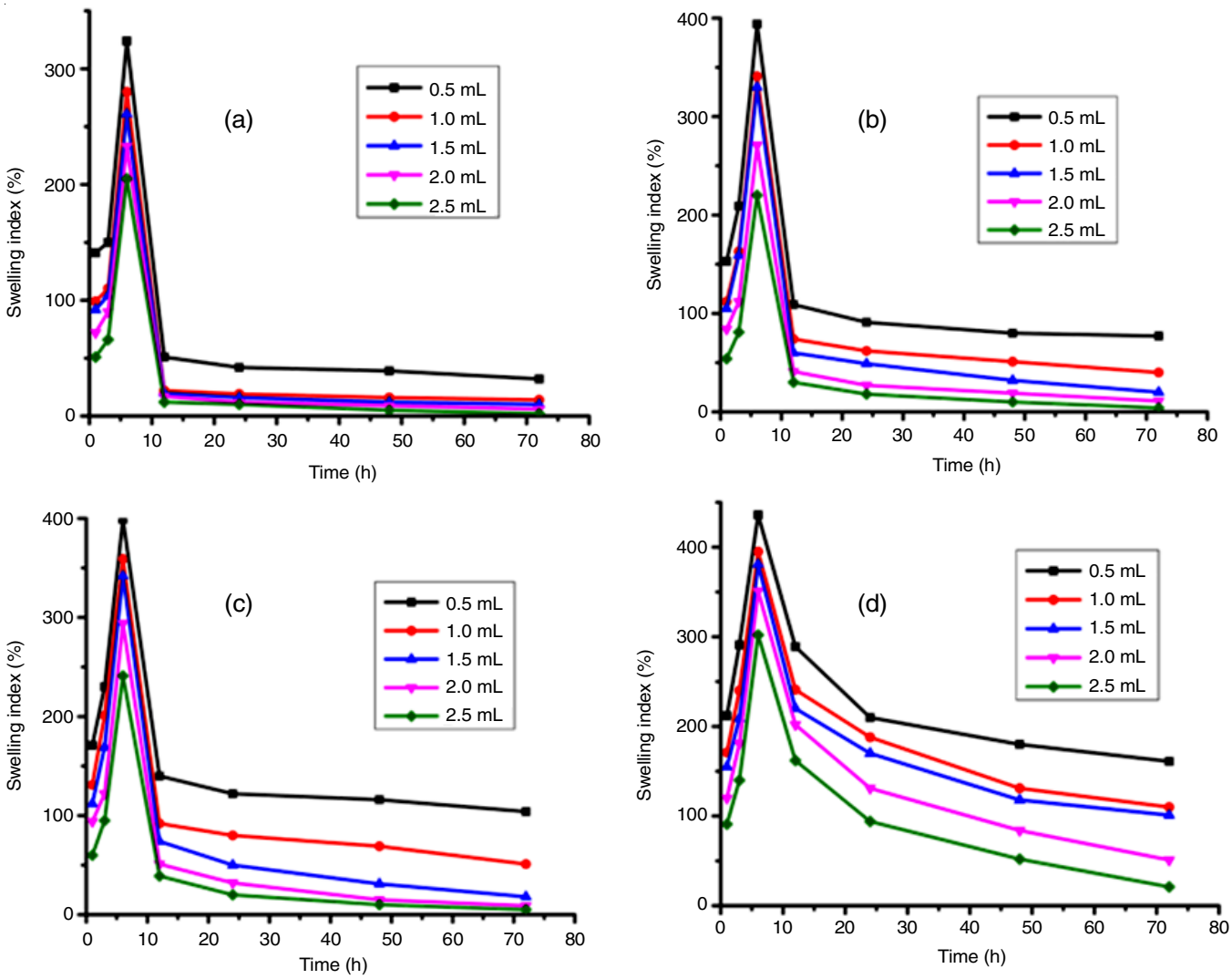

Fig. 8. Variation of swelling index (%) of coacervate with varying amounts of glutaraldehyde at (a) pH 4, (b) pH 7, (c) pH 7.4 and (d) pH 9

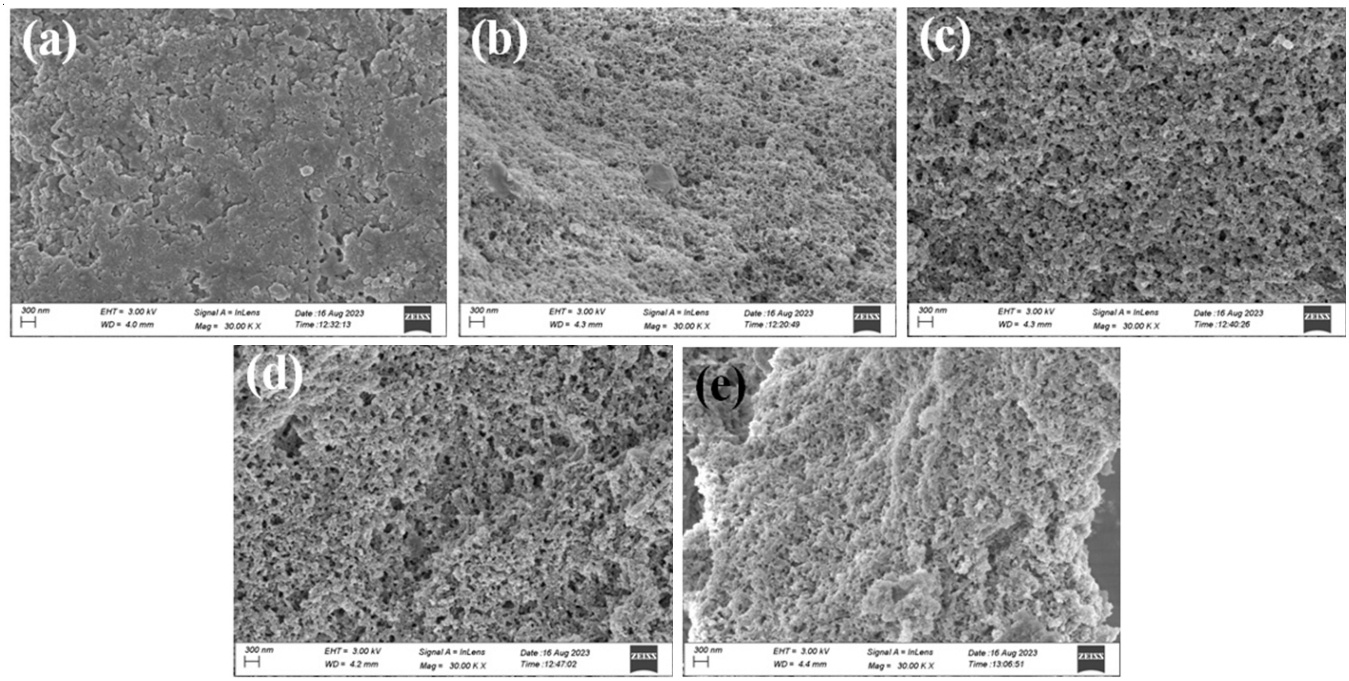

Fig. 9. Scanning electron micrographs of chitosan phosphate/κ-carrageenan coacervate crosslinked with different amounts of glutaraldehyde (a) 0.5 mL (b) 1 mL (c) 1.5 mL (d) 2 mL and (e) 2.5 mL

efficiency. An increase in the amount of glutaraldehyde results in the increases the compactness of the coacervates which reduces the capability of loading of peppermint oil, which is evident from the data given in Table-1 (entry no. 5 to 8). This, however, provides an opportunity to modulate the encapsulated amount of peppermint oil as per requirements.

Release study: Release of peppermint oil from the oil loaded coacervates was investigated at pH 4, 7, 7.4, 9. The release of peppermint oil was pH dependent and the pH dependency parallels the swelling behaviour. Release % was found to be maximum at pH 9 and minimum at pH 4. This is related to the compactness of the coacervates, which is also pH dependent. The % release against the time at four different pH are presented in Fig. 10. Initially up to 24 h , the release is fast and then it slows down and eventually attains an equilibrium after 24 h up to 72 h. The initial burst release may be related to increased diffusive loss of peppermint oil at the beginning caused by higher amount of loaded oil. Another reason may be that some amount of oil may remain adsorbed on the surface of the coacervate which is released at a faster rate at the initial stage.

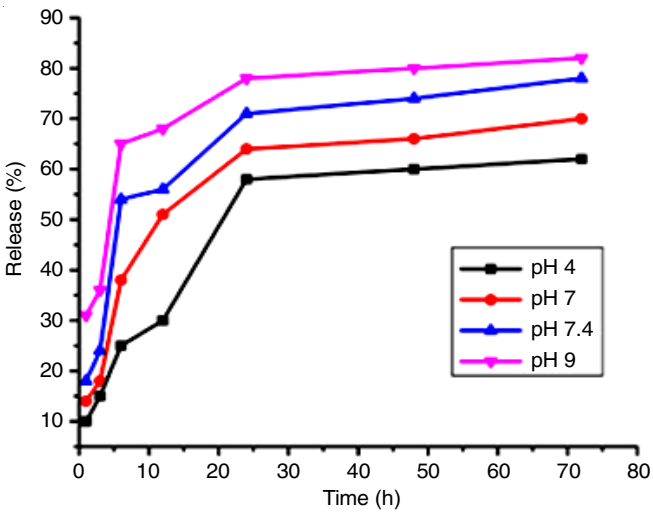

Fig. 10. % Release of peppermint oil from the peppermint oil loaded coacervate at pH 4, 7, 7.4 and 9

SEM study: A scanning electron microscope (Model Zeiss, SIGMA-300) operating at an accelerated voltage of 5 kV was used to record the SEM images of the coacervate and peppermint oil loaded coacervates. The surfaces of the samples were coated with gold before SEM analysis. The scanning electron micrographs of the pristine coacervate and peppermint oil loaded coacervate are shown in Fig. 11. The morphology of the pristine coacervate underwent a distinct change on encapsulation of peppermint oil. The pristine coacervate had a smooth morphology consisting of small sized particles. On the other hand, encapsulation resulted an increase of the particle sizes giving the impression of a rugged surface.

Antibacterial studies: The antibacterial study of peppermint oil loaded coacervate against *Proteus vulgarus*, *Klebsiella pneumonia*, *Staphylococcus epidermidis*, *Micrococcus luteus* and *Escherichia coli* were carried out in this study. The zone of inhibition of peppermint oil loaded coacervate and the positive and negative controls against those five bacterial strains are presented in Table-2. The peppermint oil loaded coacervate showed mild antibacterial activity against all the five bacterial strains with highest activity against the *Escherichia coli*.

Conclusion

The main focus of this work is the successful preparation of the complex coacervate from two biodegradable polysaccharides, a chitosan derivative and κ-carragenan, which is a regul-

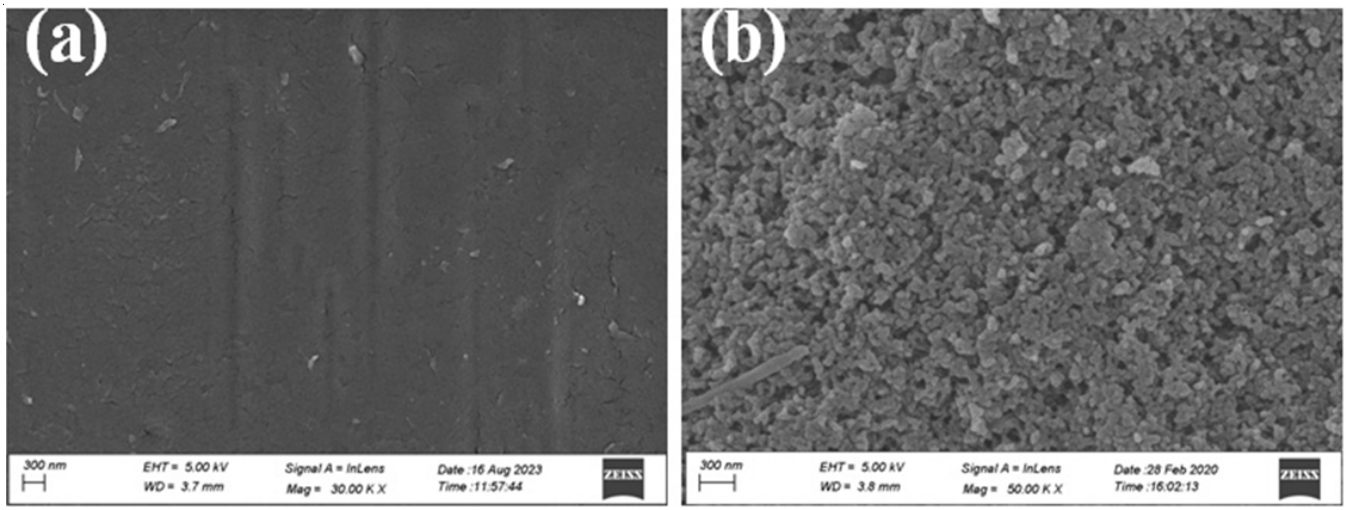

Fig. 11. Scanning electron micrographs of (a) pristine coacervate and (b) peppermint oil loaded coacervate

TABLE-2
ZONE OF INHIBITION OF CURCUMIN LOADED COACERVATE

Microorganisms	Types of microorganisms	Diameter of zone of inhibition (mm)		
		Peppermint oil loaded coacervate	DMSO	Tetracycline disc
Micrococcus luteus	Gram-positive bacteria	12.49 (± 0.45)	–	17.44 (± 0.45)
Staphylococcus epidermidis	Gram-positive bacteria	11.19 (± 0.39)	–	18.83 (± 0.25)
Escherichia coli	Gram-negative bacteria	14.94 (± 0.25)	–	13.49 (± 0.35)
Klebsiella pneumoniae	Gram-negative bacteria	13.00 (± 0.29)	–	22.96 (± 0.57)
Proteus vulgarus	Gram-negative bacteria	10.94 (± 0.19)	–	12.11 (± 0.37)

arly utilized carrier for drugs and other bioactive compounds. Further in this study commonly used chitosan is replaced by its derivative chitosan phosphate, having better aqueous solubility than chitosan. The coacervate was successfully used to encapsulate peppermint oil with a maximum loading efficiency of 84.19%. The release of peppermint oil was pH dependent and it showed a sustained release up to 72 h. Encapsulating peppermint oil in a chitosan phosphate/κ-carragenan coacervate not only allows for pH-dependent controlled release, but also preserves the oil from environmental degradation. Further variation in the amount of crosslinker in the preparation of coacervates opened up a possibility of modulating the loading efficiency of peppermint oil. The peppermint oil loaded coacervates showed mild antibacterial activity against five different bacterial strains (*Micrococcus luteus*, *Escherichia coli*, *Klebsiella pneumonia*, *Staphylococcus epidermidis* and *Proteus vulgarus*) with highest activity against *Escherichia coli*. This may provide an opportunity for its use as food antimicrobial.

CONFLICT OF INTEREST

The authors declare that there is no conflict of interests regarding the publication of this article.

REFERENCES

1. M. Tafrihi, M. Imran, T. Tufail, T.A. Gondal, G. Caruso, S. Sharma, R. Sharma, M. Atanassova, L. Atanassov, P.V.T. Fokou and R. Pezzani, *Molecules*, **26**, 1118 (2021); https://doi.org/10.3390/molecules26041118
2. M. Moghaddam, M. Pourbaige, H.K. Tabar, N. Farhadi and S.M.A. Hosseini, *J. Essen. Oil Bearing Plants*, **16**, 506 (2013); https://doi.org/10.1080/0972060X.2013.813265
3. N. Alammar, L. Wang, B. Saberi, J. Nanavati, G. Holtmann, R.T. Shinohara and G.E. Mullin, *BMC Complement. Altern. Med.*, **19**, 21 (2019); https://doi.org/10.1186/s12906-018-2409-0
4. M.S. Alam, P.K. Roy, R. Miah, S.H. Mollick, M.R. Khan, C. Mahmud and S. Khatun, *Mymensingh Med. J.*, **22**, 27 (2013).
5. N.E. Ertürk and S. Tasci, *Complement. Ther. Med.*, **56**, 102587 (2021); https://doi.org/10.1016/j.ctim.2020.102587
6. X. Liu, F. Xue and B. Adhikari, *Sustain. Food Technol.*, **1**, 426 (2023); https://doi.org/10.1039/D3FB00004D
7. Z.J. Dong, A. Toure, C.S. Jia, X.M. Zhang and S.Y. Xu, *J. Microencapsul.*, **24**, 634 (2007); https://doi.org/10.1080/02652040701500632
8. J. Yang and O.N. Ciftci, *Food Res. Int.*, **87**, 83 (2016); https://doi.org/10.1016/j.foodres.2016.06.022
9. Z. Dong, Y. Ma, K. Hayat, C. Jia, S. Xia and X. Zhang, *J. Food Eng.*, **104**, 455 (2011); https://doi.org/10.1016/j.jfoodeng.2011.01.011
10. N. Kasiri and M. Fathi, *Cellulose*, **25**, 319 (2018); https://doi.org/10.1007/s10570-017-1574-5
11. C. Deka, D. Deka, M.M. Bora, D.K. Jha and D.K. Kakati, *J. Drug Deliv. Sci. Technol.*, **35**, 314 (2016); https://doi.org/10.1016/j.jddst.2016.08.007
12. S. Ghayempour and M. Montazer, *Carbohydr. Polym.*, **205**, 589 (2018); https://doi.org/10.1016/j.carbpol.2018.10.078
13. C. Liu, M. Li, N. Ji, J. Liu, L. Xiong and Q. Sun, *J. Agric. Food Chem.*, **65**, 8363 (2017); https://doi.org/10.1021/acs.jafc.7b02938
14. A. Shetta, J. Kegere and W. Mamdouh, *Int. J. Biol. Macromol.*, **126**, 731 (2019); https://doi.org/10.1016/j.ijbiomac.2018.12.161
15. H. Parkzad, I. Alemzadeh and A. Kazemi, *J. Int. Eng. Trans. B Appl.*, **26**, 807 (2013).
16. G. Huang, Y. Liu and L. Chen, *Drug Deliv.*, **24**, 108 (2017); https://doi.org/10.1080/10717544.2017.1399305
17. C. Deka, L. Aidew, N. Devi, A.K. Buragohain and D.K. Kakati, *J. Biosci.*, **27**, 1659 (2016); https://doi.org/10.1080/09205063.2016.1226051

18. B.K. Sridhar, A. Srinatha and M.S. Khan, *Indian J. Pharm. Sci.*, **72**, 18 (2010); https://doi.org/10.4103/0250-474X.62230
19. R.K. Das, N. Kasoju and U. Bora, *Nanomedicine*, **6**, 153 (2010); https://doi.org/10.1016/j.nano.2009.05.009
20. J. Hudzicki, Kirby-Bauer Disk Diffusion Susceptibility Test Protocol, American Society for Microbiology (2016).
21. S. Phongpaichit, J. Nikom, N. Rungjindamai, J. Sakayaroj, N. Hutadilok-Towatana, V. Rukachaisirikul and K. Kirtikara, *FEMS Immunol. Med. Microbiol.*, **51**, 517 (2007); https://doi.org/10.1111/j.1574-695X.2007.00331.x
22. M. Fernandes Queiroz, K. Melo, D. Sabry, G. Sassaki and H. Rocha, *Mar. Drugs*, **13**, 141 (2015); https://doi.org/10.3390/md13010141
23. W.A.K. Mahmood, M.M.R. Khan and T.C. Yee, *J. Phys. Sci.*, **25**, 123 (2014).
24. N. Pramanik, D. Mishra, I. Banerjee, T.K. Maiti, P. Bhargava and P. Pramanik, *Int. J. Biomater.*, **2009**, 1 (2009); https://doi.org/10.1155/2009/512417
25. M. Yilmaztekin, S. Levic, A. Kaluševic, M. Cam, B. Bugarski, V. Rakic, V. Pavlovic and V. Nedovic, *J. Microencapsul.*, **36**, 109 (2019); https://doi.org/10.1080/02652048.2019.1607596
26. M.E.I. Badawy, N.E.M. Taktak, O.M. Awad, S.A. Elfiki and N.E.A. El-Ela, *J. Macromol. Sci. B Phys.*, **56**, 359 (2017); https://doi.org/10.1080/00222348.2017.1316640
27. R.M. Silverstein, G.C. Bassler and T.C. Morrill, Spectroscopic Identification of Organic Compounds, edn. 5, John Wily & Sons: New York (1981).
28. S. Kumar and J. Koh, *Int. J. Mol. Sci.*, **13**, 6102 (2012); https://doi.org/10.3390/ijms13056102
29. N. Al-Zebari, S.M. Best and R.E. Cameron, *J. Phys. Mater.*, **2**, 015003 (2019); https://doi.org/10.1088/2515-7639/aae9ab
30. T.N. Carneiro, D.S. Novaes, R.B. Rabelo, B. Celebi, P. Chevallier, D. Mantovani, M.M. Beppu and R.S. Vieira, *Macromol. Biosci.*, **13**, 1072 (2013); https://doi.org/10.1002/mabi.201200482
31. S. Distantina, R. Rochmadi, M. Fahrurrozi and W. Wiratni, *Eng. J.*, **17**, 57 (2013); https://doi.org/10.4186/ej.2013.17.3.57